Substrate Defects and Variations in Interfacial Ordering of Monolayer Molecular Films on Graphite

David L. Patrick and Thomas P. Beebe, Jr.*

Department of Chemistry, The University of Utah, Salt Lake City, Utah 84112

Received August 11, 1993. In Final Form: October 19, 1993®

Scanning tunneling microscopy is used to investigate monolayer films of the liquid crystal 4'-octyl-4-biphenylcarbonitrile (8CB) deposited onto highly ordered pyrolytic graphite. These self-assembled films display a wide variety of structural forms, several of which are reported here for the first time. Nanometer-resolution images provide insight into the important molecule–molecule and molecule–substrate interactions determining film structure. The role of substrate defects in determining interfacial order is discussed, and a growth mechanism is proposed to account for the infrequent observation of certain monolayer film structures reported here.

Introduction

Surface ordering in thin films has been studied for a number of years due to its importance for technologies, such as high-performance liquid crystal displays, and for scientific understanding, as a model for a variety of fundamental and applied interfacial phenomena.[1] For technological applications, accurate control of film chemical and physical properties is of great concern, as is the complexity of the manufacturing process. As a result, films composed of self-assembling molecules have received increased attention in recent years; their ease of preparation and the large number of molecules from which they can be formed make them promising candidates for use in devices based on thin film technology.[2]

Much of the activity in the field of self-assembled films (SAFs) has been directed toward the search for a better understanding of the connection between molecular structure and film morphology. The roles of chemical functionalities, constituent molecule size and shape, as well as the influence of the substrate on which the film is grown have all been examined for their contributions to SAF structure.

SAFs formed from liquid crystalline materials have received considerable attention in this regard, since their bulk properties are well known and they readily self-assemble into ordered layers. In particular, the homologous *n*-alkylcyanobiphenyl (*m*CB *m* = 6–12) series of liquid crystals has been studied in detail, with films grown on several different substrates.[3-6] However, attempts to find trends suggesting connections between molecular structure and film morphology from analysis of the different two-dimensional crystalline patterns formed by these molecules are complicated by the fact that at least one of them (8CB) can form more than one stable pattern. In order to formulate a better understanding of molecular structure–film morphology relationships, it is first necessary to explain natural variations within the members of the series. In this paper, we report nanometer-resolution structural studies of ordered 8CB films grown on highly ordered pyrolytic graphite (HOPG) using scanning tunneling microscopy (STM). We describe four previously unknown molecular packing arrangements and propose a growth mechanism linking adsorbate structural polymorphism to substrate defects. The effect of temperature on film growth is also discussed.

Experimental Section

The STM used in these studies is custom built and described elsewhere.[7] All images were acquired in air at room temperature using mechanically cut Pt/Rh tips (20% Rh). The liquid crystal used was 4'-octyl-4-biphenylcarbonitrile (8CB) which exists as a smectic-A_2 phase near room temperature in bulk form and has $S_a \rightarrow N$ and $N \rightarrow I$ transition temperatures of 21 and 40 °C, respectively. 8CB was used as received from Aldrich Chemical

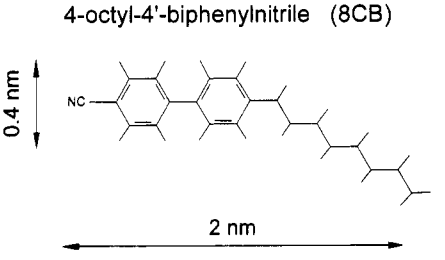

Corp. (99%). Samples were prepared by applying a ~20-μL drop of 8CB as a neat liquid to a freshly cleaved HOPG surface, heating to >10 °C above the isotropic transition temperature (~50 °C) of the liquid crystal for ~15 min, and slowly cooling for ~30 min. This preparation procedure produces effective surface ordering of liquid crystals approximately 75% of the time within 30 min of reaching room temperature. If samples are not heated, crystallization still occurs, but over a period of days. Except where noted, all images reported here were acquired using constant-height mode and are unprocessed except for least-

* Author to whom correspondence should be addressed.

® Abstract published in *Advance ACS Abstracts*, December 1, 1993.

(1) Brown, G. H.; Doane, J. W. *Appl. Phys.* **1974**, *4*, 1.

(2) *Nanotechnology*, Crandall, B. C., Lewis, B. C., Eds.; MIT Press: Cambridge, MA, 1989.

(3) Smith, D. P. E.; Heckl, W. M. *Nature* **1990**, *346*, 616. Iwakabe, Y.; Hara, M.; Kondo, K.; Tochigi, K.; Mukoh, A.; Yamada, A.; Garito, A. F.; Sasabe, H. *Jpn. J. Appl. Phys.* **1991**, *30* (10), 2542. Mizutani, W.; Shigeno, M.; Sakakibara, Y.; Kajimura, K.; Ono, M.; Tanishima, S.; Ohno, K.; Toshima, N. *J. Vac. Sci. Technol.* **1990**, *A8*, 675. Hara, M.; Iwakabe, Y.; Tochigi, K.; Sasabe, H.; Garito, A. F.; Yamada, A. *Nature* **1990**, *344*, 228. Mizutani, W.; Shigeno, M.; Ohmi, M.; Suginoya, M.; Kajimura, K.; Ono, M. *J. Vac. Sci. Technol.* **1991**, *B9* (2), 1102. Shigeno, M.; Ohmi, M.; Suginoya, M.; Mizutani, W. *Mol. Cryst. Liq. Cryst.* **1991**, *199*, 141. Mizutani, W.; Shigeno, M.; Ono, M.; Kajimura, K. *Appl. Phys. Lett.* **1990**, *56* (20), 1974. Iwakabe, Y.; Hara, M.; Kondo, K.; Tochigi, K.; Mukoh, A.; Garito, A. F.; Sasabe, H.; Yamada, A. *Jpn. J. Appl. Phys.* **1990**, *29* (12), L2243.

(4) Foster, J. S.; Frommer, J. E.; Spong, J. K. *SPIE* **1989**, *1080*, 200.

(5) McMaster, T. J.; Carr, H.; Miles, M. J.; Cairns, P.; Morris, V. J. *Liq. Cryst.* **1991**, *9* (1), 11. McMaster, T. J.; Carr, H.; Miles, M. J.; Cairns, P.; Morris, V. J. *J. Vac. Sci. Technol.* **1990**, *A8*, 672.

(6) Smith, D. P. E.; Höber, J. K. H.; Binnig, G.; Nejoh, H. *Nature* **1990**, *344*, 641. Nejoh, H. *Appl. Phys. Lett.* **1990**, *57*, 2907.

(7) Lyding, J. W.; Skala, S.; Hubacek, J. S.; Brockenbrough, R.; Gamie, G. J. *J. Microsc. (Oxford)* **1988**, *152*, 371. Zeglinski, D. M.; Ogletree, D. F.; Beebe, T. P., Jr.; Hwang, R. Q.; Somorjai, G. A.; Salmeron, M. B. *Rev. Sci. Instrum.* **1990**, *61*, 3769.

0743-7463/94/2410-0298$04.50/0

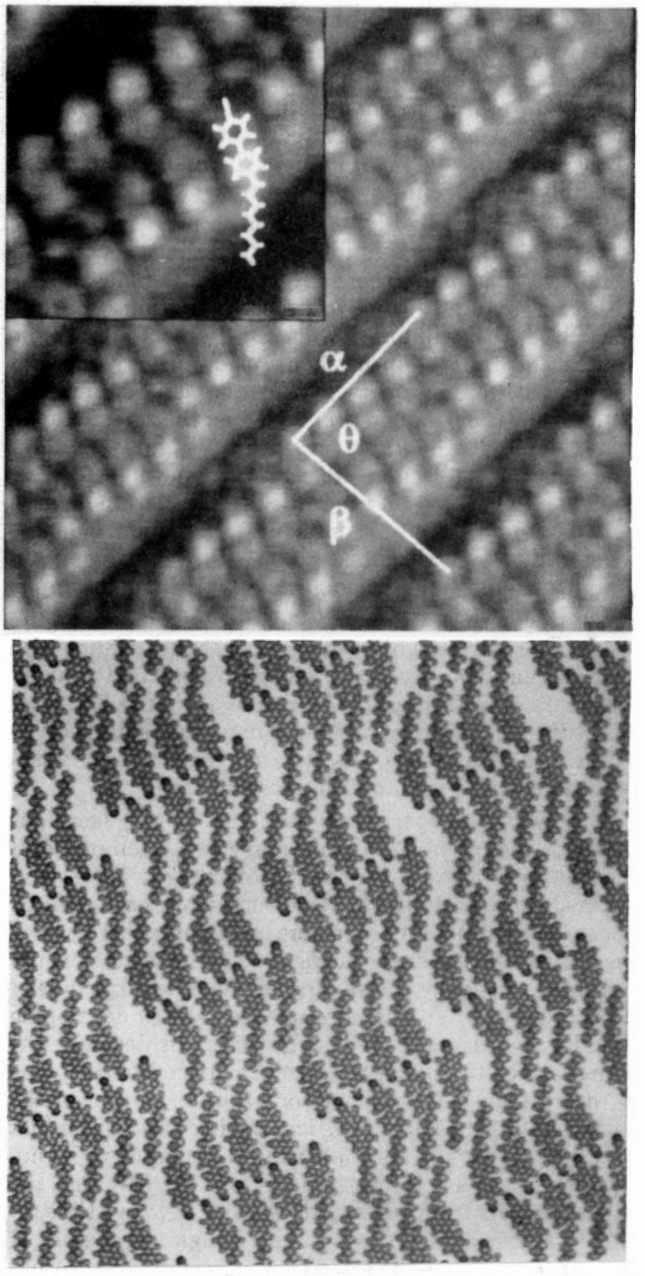

Figure 1. (a, top) 95 Å × 95 Å constant height image of one of the "standard" 8CB structures on HOPG. Inter-row spacing is 33 Å. $V_b = -0.55$ V (sample negative relative to the tip). Values for α, β, and θ are reported in Table 1. Image produced by pixel-wise averaging five images, individually corrected for thermal drift. Figure inset shows a single unit cell with the position of one molecule marked by a model overlay. (b, bottom) Model of structure in part a. Model size is approximately the same as the image.

squares image plane subtraction to account for sample "tilt". Figures 1–4 are pixel-wise averages of complementary left and right pages. The images presented here use a false color scale with brighter colors corresponding to higher tunneling current. Model structures were generated using a commercially available software visualization and modeling package (HyperChem by Autodesk, Inc., Marin, CA).

Results and Discussion

1. Structural Variations. The structure shown in Figure 1a, which we refer to as the "standard structure", has been widely observed and reported and occurs far more frequently than any other. This configuration is actually one example of a group of related structures, each bearing a strong similarity to the others. The standard structure is formed from unit cells with eight molecules arranged in a double-row or "bilayer" configuration, as shown in the model of Figure 1b. The side-to-side distance between molecules may be either 4.3 or 6.4 Å, a difference of one graphite period. The inter-row spacing ($= \beta \cos(90 - \theta)$, where β and θ are defined in Figure 1a) can vary from 32 to 54 Å, with spacings of 37 and 40 Å observed most frequently. When the inter-row spacing is ~38 Å or less, the molecules pack 4.3 Å side-to-side; between ~38 and ~44 Å, the molecules are spaced further apart at 6.4 Å. In structures with spacings greater than this amount, the unit cell changes in a way that is not currently understood. The various spacings that have been observed with this general pattern of molecules collectively make up the family of "standard structures". See Table 1 for a detailed analysis of unit cells.

In all versions of the standard structure, high-resolution images indicate that the cyanobiphenyl "heads" of the molecules splay apart within the unit cell to minimize repulsive side-to-side interactions, although the alkyl "tails" remain parallel and anchored in place at 4.3- or 6.5-Å intervals. This splayed geometry causes a progressive increase in the intramolecular head–tail angles in molecules within one unit cell, resulting in a periodic dislocation of the unit cell in a direction transverse to the rows, every fourth molecule to alleviate steric strain (see the dimension α in Figure 1a).

The interactions acting in each member of the family of standard structures are evidently very similar. These types of staggered bilayer patterns (which are also formed[8] by 10CB and 12CB) strongly resemble the configuration of molecules in a cross section of the bulk smectic C̃ phase, sometimes called a "frustrated" smectic. The smectic C̃ phase arises from competing intermolecular interactions, each tending to orient the molecules in a slightly different way.[9] Many molecules that form the smectic C̃ phase contain two polar groups, one whose dipole is directed along the axis of the molecule and the other whose dipole is transverse to it.[10] The staggered bilayer pattern in these smectic C̃ phases represents a compromise between two strong dipole–dipole interactions.

Molecular patterns like the one in Figure 1 can be explained in similar terms. The most highly ordered bulk phase of 8CB is the smectic A_2 phase, which is a bilayer configuration formed by strong dipole–dipole interactions along the axis of the molecule. However, 8CB also interacts fairly strongly with an HOPG surface (please see ref 11), resulting in a competition between alignment forces for molecules near the substrate. The intermolecular dipole–dipole interactions responsible for bulk ordering compete with molecule–surface forces (operating in a transverse direction) to form a pattern representing a compromise of the two.

Although the standard structures are qualitatively similar, 8CB will occasionally form patterns that are very different. Figure 2 shows a crystalline pattern which differs

(8) Smith, D. P. E.; Heckl, W. M.; Klagges, H. A. *Surf. Sci.* **1992**, *166*, 278.

(9) Prost, J.; Barois, P. *J. Chim. Phys.* **1983**, *80*, 65.

(10) Gray, G. W.; Goodby, J. W. G. *Smectic Liquid Crystals*; Leonard Hill Inc.: 1984; p 143.

(11) Preliminary results from temperature programmed desorption experiments performed in ultrahigh vacuum on thin films (100–200 Å) of 8CB grown by sublimation onto graphite indicate that the first monolayer is bound to the surface by ~36 kcal/mol and successive layers by ~21 kcal/mol. During review, it was pointed out that the anisotropic part of the surface–molecule interaction plays the greatest role in determining film structure and that desorption energies measured by temperature programmed desorption are not directly relevant. For many systems however, the two are approximately related by $E_{diffusion} \approx E_{desorption}/4$, where the activation energy for diffusion, $E_{diffusion}$, is the anisotropic portion of the interaction energy between an adsorbate and substrate (Adamson, A. W. *Physical Chemistry of Surfaces*; John Wiley & Sons: New York, 1990).

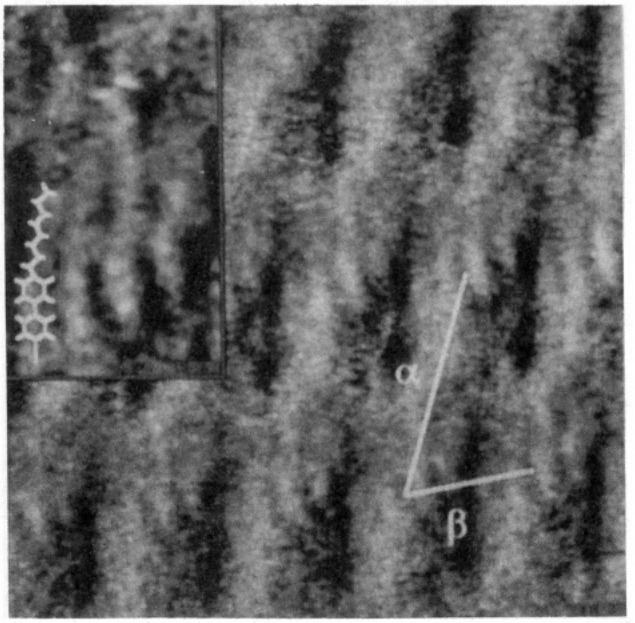

Figure 2. 125 Å × 125 Å constant height image. V_b = −0.77 V. Each unit cell contains four highly ordered molecules (visible as closely spaced parallel lines) with three to four disordered ones (in the "blurred" regions). This image is a pixel-wise average of four images, individually corrected for drift. The image-averaging process enhances the appearance of the four ordered molecules (which remain fixed in position relative to one another during the acquisition of individual images), although the disordered ones, whose positions change during image acquisition, appear indistinct. Figure inset shows a single unit cell with the position of one molecule marked by a model overlay. Unit cell vectors (Table 1) are indicated in white.

from the standard structures in one important way. In all other reported examples of liquid crystal monolayers observed by STM, including those presented here, the molecules have been observed to form periodic assemblies with both short-range and long-range crystalline order. We interpret the structure shown in Figure 2, however, as one in which short-range disorder occurs periodically within an otherwise highly ordered lattice. This interpretation arises from analysis of a series of images revealing that part of the unit cell contains molecules in a somewhat disordered state. Disordered regions appeared "blurred" in the STM images and occupy approximately half the each unit cell while other parts of the unit cell are simultaneously imaged more clearly. The number, precise position, and orientation of molecules in this region differ from unit cell to unit cell and appear to change with time. Molecules in the upper half of the unit cell, however, are highly ordered and close-packed side to side.

Figure 2 is a pixel-wise average of four individual images, taken one after another over a period of several minutes. Combining successive images in this way enhances features that remain constant while deemphasizing those that change on the time scale of one image. The resulting composite image shows four well-defined molecules along with an indistinct region in each unit cell. Recent work by Askadskaya and Rabe[12] suggests that long-chain *n*-alkanes on HOPG can exhibit diffusional disorder or short range diffusional motion during the STM image time scale. The result is a similar blurred region in the STM image, which represents an average over the molecular positions during acquisition.

The existence of a stable molecular assembly combining short-range ordered and disordered elements within a long-range periodic framework is surprising when considered against the large number of self-assembled monolayers now studied by microscopic methods. Point defects and disordered regions are notably infrequent in other similar systems. From a thermodynamic standpoint, however, the increased entropy associated with disordered regions of the structure in Figure 2 may help to stabilize the assembly by reducing its overall free energy.

The structures in Figures 1 and 2, along with those reported by other workers, indicate the variety of molecular packing arrangements that can occur on different samples. Although unlikely, some of these variations may be attributed to small, unintentional differences in sample or surface preparation methods. However, the second group of structures presented in this paper shows that structural variations can occur even on the same sample, under identical preparation conditions. Figures 3–5 show three distinct molecular arrangements never before reported, all observed on the same sample, within an area less than 1 μm^2. The area outside of this small region was covered by one of the standard structures, giving a total of four different patterns observed on the same sample.

The first of these three new structures is shown in Figure 3a. The bright, roughly oval regions are consistent with a model that places molecules head-to-head and grouped into pairs, as indicated in the model of Figure 3b. This structure has the lowest molecular density of any observed so far (see Table 1) and is the only structure in which repulsive side-to-side interactions are absent.

The second new structure observed on this sample is shown in Figure 4. In this case, repeated attempts to fit the patterns shown in the STM images to a two-dimensional collection of 8CB molecules were unsuccessful. For each attempted fit, there were inevitably areas in which the cyanobiphenyl heads of one group of molecules would be forced to occupy the same spaces as the alkyl tails of another group. We were also unsuccessful at developing a model that places the molecules on their sides (with the plane formed by the biphenyl group normal to the plane of the surface) due to steric constraints. Images of the pattern in Figure 4 are of sufficiently high resolution that they should permit an approximate assignment of molecular positions and orientation. It is unlikely that the pattern results from an imaging artifact (*e.g.*, multiple tip effect), since a "defect" row runs through two regions of the image and since the same tip was used to image other 8CB structures, including the standard structure. In Figure 5, for example, two structures are shown simultaneously (refer to figure caption). Alternatively, the molecular pattern in Figure 4 may arise from a layered configuration of molecules, as has been recently observed by STM for some alkanes.[13] If so, a simple two-dimensional interpretation of the molecular positions would fail to give an adequate description. The third new structure observed on this sample is shown in a central swath of Figure 5. Images of this complex assembly lack sufficient resolution to allow a structural interpretation at this time.

2. Formation Mechanism. Interfacial ordering of liquid crystals is influenced not only by molecule–molecule and molecule–substrate interactions but also by the mechanical and thermal history of the sample. The procedure used for substrate preparation, for example "rubbing", can significantly affect the surface structure of liquid crystal films.[14] The samples on which the new and unusual structures reported here occurred, however, were prepared in the same way as dozens of other samples on which only the standard structure was observed.

(12) Askadskaya, L.; Rabe, J. P. *Phys. Rev. Lett.* **1992**, *69*, 1395.

(13) Watel, G.; Thibaudau, F.; Cousty, *Surf. Sci. Lett.* **1993**, *281*, L297.

(14) Berreman, D. W. *Phys. Rev. Lett.* **1972**, *28*, 1683.

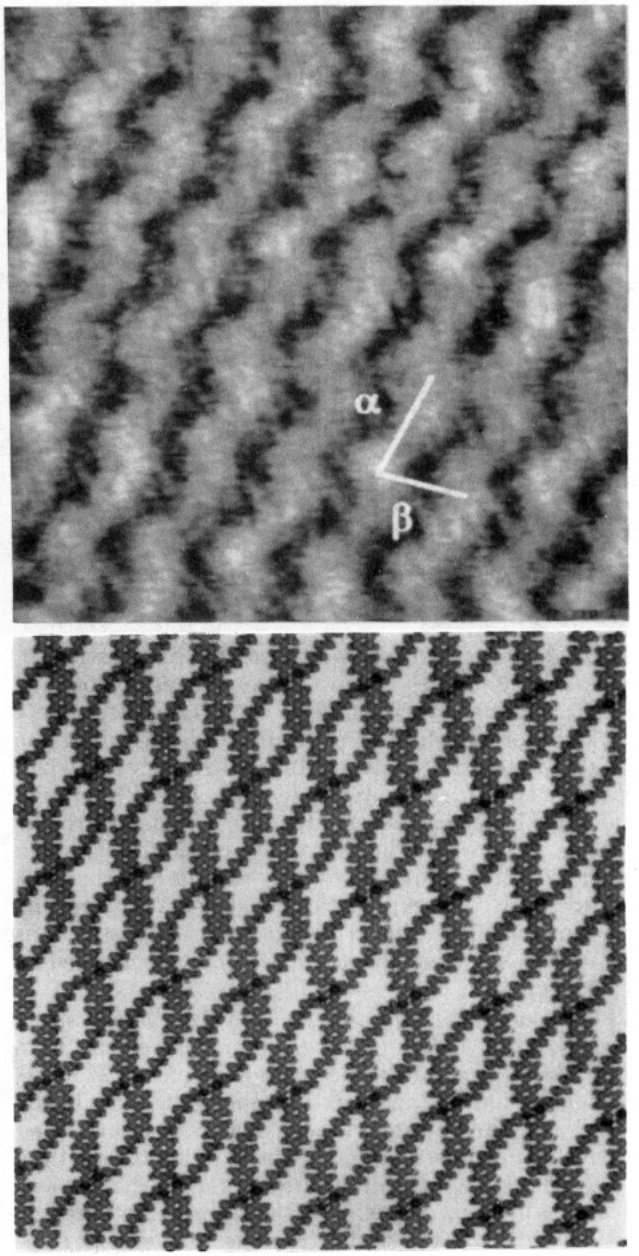

Figure 3. (a, top) 125 Å × 125 Å constant height image. V_b = −0.70 V. Each of the bright elliptical regions contains two cyanobiphenyl head groups. Unit cell vectors (Table 1) are indicated in white. (b, bottom) Model of structure in part a. Model size is approximately the same as the image.

Table 1. Summary of 8CB Molecular Packing Unit Cell Structures and Surface Densities

	Figure 1[e]	Figure 2[d]	Figure 3[d]	Figure 4[d]	Figure 5[d]
α (Å)[a]	33	46	21	53	48
β (Å)[a]	35	26	16	12	35
θ (deg)[a]	72	68	74	88	109
molecules/unit cell	8	7–8[b]	2	6	–[c]
molecules/cm² (×10¹³)	7.2	6.7	6.2	9.4	–[c]

[a] α, β, and θ refer to the dimensions of each unit cell as indicated in Figures 2–7. [b] Due to the inherent disorder in this structure, the number of molecules per unit cell is not constant. [c] The structure within the unit cell was not determined due to its complexity and resolution of the images. Unit cell dimensions are reported here for the benefit of those interested in further studies. [d] ±10%. [e] ±5%.

It has been suggested that the thermal history of a sample (for example, its rate of cooling) can affect the crystalline structure of the resulting film.[4] To test this hypothesis, we have varied the initial and final temperatures (sample temperatures during 8CB application and imaging, respectively) and the rate of cooling. Initial temperatures were varied from 20 to 50 °C, final temperatures from 20 to 35 °C, and cooling rates between 0 and ~200 °C min^{-1}. We have found that high cooling rates initially reduce the percentage of surface area covered by an ordered film but do not otherwise affect film structure. Initial and final temperatures also have surprisingly little effect on the details of the packing arrangement, although samples prepared and imaged at room temperature show a greater percentage of grain boundaries and similar defects than those that are heated.

The only apparent distinguishing feature between these and other samples was the nature of the substrate topography in the vicinity of the new structures.[15] Figure 6 illustrates this for a sample on which one group of new

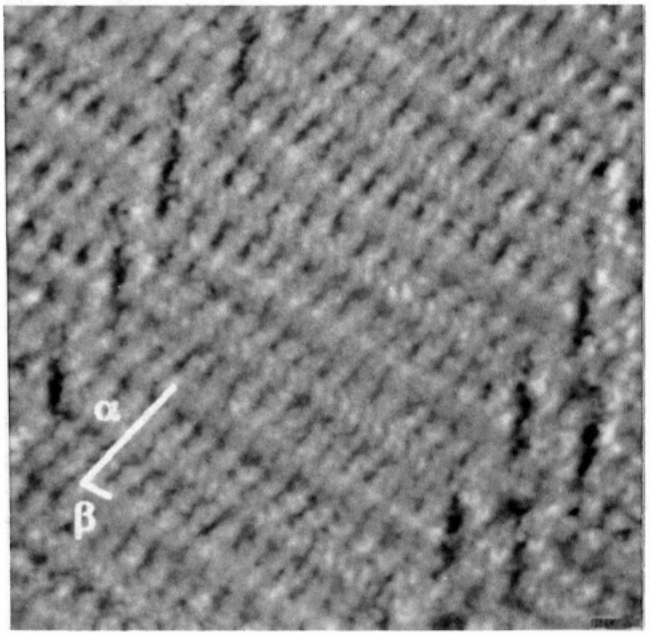

Figure 4. 220 Å × 220 Å constant height image. Unit cell vectors (Table 1) are indicated in white. V_b = −0.70 V.

Figure 5. 425 Å × 425 Å constant height image showing two molecular patterns occupying adjacent areas of a graphite surface. One of the two structures is seen in more detail in Figure 4. Unit cell vectors for the other are indicated in white. Images of this structure lack sufficient resolution to propose a model at this time. V_b = −0.70 V.

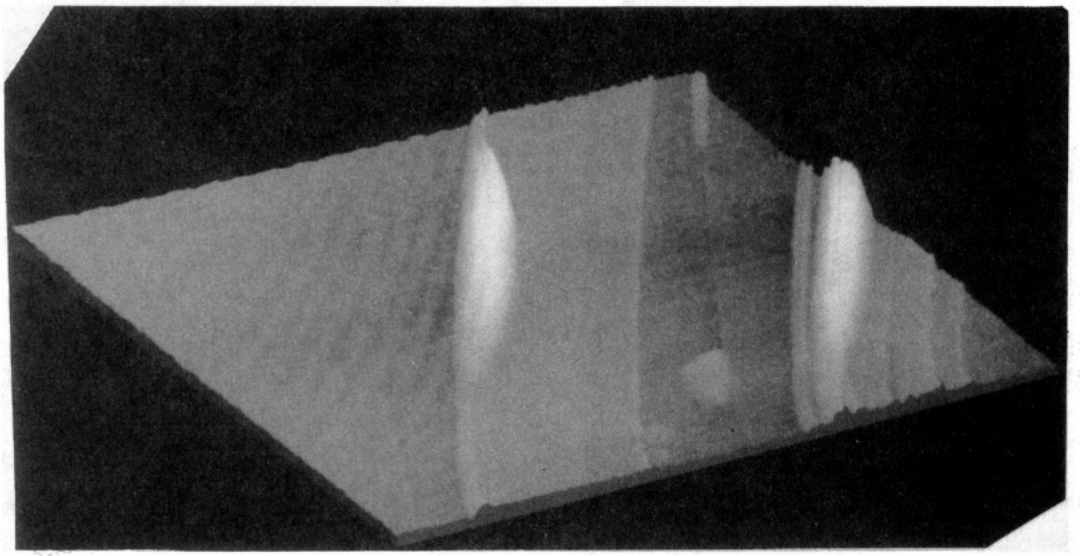

Figure 6. 7000 Å × 7000 Å × 125 Å constant current image of sample topography around the region containing the unusual structures shown in Figures 2–5. V_b = −0.48 V.

structures (Figures 3–5) was observed. In this case, the unusual structures were found in a roughly rectangular region 6000 Å wide and ~2 μm long, *bordered on each side* by multiple atomic steps on the graphite substrate. The area within the rectangular region was further subdivided into several terraces separated by single atomic steps. It was on these terraces that the new structures were observed. The entire surface for several thousand angstroms in every direction *outside* of the rectangular region was covered by the standard structure, and this structure was not observed within the rectangular region.

It is unlikely that graphite step defects contributed directly to the formation of the unusual structures reported here. We have repeatedly observed that such features cause only minor perturbations in film structure on other samples, and Smith has reported the presence of the standard structure on terraces as narrow as 60 Å.[16] Instead, we suggest the defects *preserved* the unusual structures once they had formed, allowing them to persist long enough to be imaged with STM.

Evidence for this preservation mechanism comes from consideration of the way crystalline domains grow across the surface after nucleation has occurred. Observations of the standard structure on several hundred different HOPG terraces reveal that (1) a terrace is either completely covered by an ordered film or not covered at all (partial coverage is never observed), (2) the structure and orientation of crystalline domains on adjacent terraces separated by one or more graphite steps is often different, and (3) molecular grain boundaries, except where associated with substrate defects, are extremely uncommon under these conditions in annealed films. These observations suggest that, typically, a single nucleation event is sufficient to tile an entire terrace with an ordered layer, although the tiling mechanism does not, in general, act across graphite steps to cover adjacent terraces. Other dynamic processes, such as grain boundary motion and large-scale molecular reorientations induced by, for example, pulsing the bias voltage, behave similarly, with effects confined to a single terrace.

If the standard structures are thermodynamically favored over the "unusual" structures reported here, they may ordinarliy be replaced, or annealed out, by the standard structures shortly after sample preparation. If, however, an unusual structure formed in a region bounded by substrate defects, the defects could act to effectively block the propagation of molecular ordering along the surface, preserving the unusual structures long enough to be imaged with STM. We note that although unusual structures have been observed in direct contact with one another, as shown in Figure 5, they have not been seen in direct contact with one of the standard structures. According to this explanation, higher-energy unusual structures would be imaged more frequently in regions bounded by substrate defects, a prediction confirmed by experiment.

The observations reported here and elsewhere of structural variation in liquid crystal monolayers may have implications for other studies. For example, STM investigations of liquid crystal mixtures should be preceded by a thorough exploration of the set of structures exhibited by each component individually in order to differentiate between native structural variations (polymorphism) and variations induced by mixing. These same variations may also explain some of the discrepancies reported in measurements of surface order parameters by different workers studying similar mesogen-substrate systems using spatially-averaging techniques.[17]

Conclusions

We have reported the observation and characterization of four previously unknown two-dimensional molecular packing arrangements of 8CB molecules on HOPG. The occurrence of these structures near substrate defects is explained by a growth mechanism in which graphite steps preserve unusual structures by preventing the encroachment of the most commonly observed molecular configuration. We have found little connection between thermal conditions during sample preparation and imaging and resulting film structure.

Acknowledgment. We thank Victor Cee and Andrew Leavitt and acknowledge the help of Dr. Russ Brown and members of The Utah Supercomputing Institute, including Dr. Julio Facelli. This work was partially supported by a grant from the NSF (CHE-9206802) and by The University of Utah. Preliminary experiments were conducted by Mr. Solomon Basame, who was supported by the NSF REU program.

(15) No large scale images of the structure in Figure 2 were acquired during the experiment, and the nature of the surrounding topography in this case in unknown.

(16) Smith, D. P. E. *J. Vac. Sci. Technol.* **1991**, *B9* (2), 1119.

(17) Jérôme, B. *Rep. Prog. Phys.* **1991**, *54*, 391.